The ENSO Cycle and Forecastability of Global Inflation and Output Growth: Evidence from Standard and Mixed-Frequency Multivariate Singular Spectrum Analyses

Hossein Hassani [a], Mohammad Reza Yeganegi[b] and Rangan Gupta[c]

[a]The Research Institute of Energy Management and Planning (RIEMP), University of Tehran, No. 9, Ghods St., Tehran, Iran;
[b]Department of Accounting, Central Tehran Branch, Islamic Azad University, Tehran, Iran;
[c]Department of Economics, University of Pretoria, Pretoria 0002, South Africa

ARTICLE HISTORY
Compiled October 14, 2021

ABSTRACT
In this paper the role of the El Niño-Southern Oscillation (ENSO), measured by the Equatorial Southern Oscillation Index (EQSOI), is used to formally forecast the inflation and GDP growth rates of the United States (US), advanced (excluding the US) and emerging countries, as well as the world economy (barring the US). We rely on univariate and multivariate Singular Spectrum Analyses (SSA), as well as mixed-frequency version of the latter since the EQSOI is monthly, while GDP is available only at quarterly frequency unlike monthly inflation rates. We find statistically significant evidence of the ability of the EQSOI in forecasting inflation and GDP growth rates of the four economic blocs, though there are exceptions in terms of forecasting gains associated with inflation rate of emerging economies and the growth rate of the US. Our results have important implications for policymakers.

KEYWORDS
GDP growth; Inflation; ENSO; Forecastibility; Mixed-Frequency Multivariate SSA; Continuous Wavelet Transform.
JEL: C22; C32; E31, E32; E37; Q54.

1. Introduction

The El Niño-Southern Oscillation (ENSO) is an irregularly periodic variation in winds and sea surface temperatures over the tropical eastern Pacific Ocean, which tends to affect the climate of much of the tropics and subtropics [30]. The warming phase of sea temperature is known as El Niño and the cooling phase as La Niña. Each of these two phases can last several months and typically occur every few years with varying intensities per phase. However, it would be a mistake to think of the ENSO as merely affecting climate patterns, but instead, some studies have highlighted its ability to produce downturn phases of the business cycle to some degree, but primarily causing inflationary impacts via increases in agricultural commodity and crude oil prices [1, 2, 5, 6, 9, 23, 25, 28], due to El Niño and La Niña events producing major global rare disaster risks historically [7, 14, 26].

While these studies are of tremendous importance in deducing the empirical link

Corresponding Author Hossien Hassani, Email: hassani.stat@gmail.com

between ENSO and major macroeconomic variables, i.e., growth and inflation, these primarily being in-sample (causal and structural) analyses are to some degree of limited value to policymakers in general, and central banks in particular, who would need accurate predictions of the future path of key economic variables, i.e., out-of-sample forecasts, while making their policy decisions, following episodes of weather-related uncertainties. Moreover, from a statistical perspective, it is well-established that in-sample predictability does not guarantee out-of-sample forecasting gains emanating from a specific predictor, besides the fact that it is out-of-sample forecasting that tends to provide a more robust test of the appropriateness of an econometric model and the predictor [3]. Given this, the objective of this paper is to provide for the first time an out-of-sample forecasting analysis of output growth and inflation based on the information content of the ENSO cycle for not only the United States (US), but also regional blocs involving other advanced (excluding the US) and emerging economies, besides the overall world (excluding the US).

In this regard, as far as the econometric model is concerned, we rely on the Multivariate Singular Spectrum Analysis (MSSA). We are motivated to use SSA because it is a non-parametric technique that works with arbitrary statistical processes, whether linear or non-linear, stationary or non-stationary, Gaussian or non-Gaussian [27], and being a versatile approach for modelling and forecasting time series, it has been found to outperform wide-array of other forecasting models [11, 15, 17, 18]. At this stage, we must also highlight that, since the ENSO data is available monthly, while the Gross Domestic Product (GDP) growth data are quarterly, we rely on a mixed-frequency MSSA model to forecast the growth rate, as recently developed by [20], rather than averaging the ENSO data over three-months forming the quarter to prevent possible loss of information [8]. This serves as an additional empirical novelty of our paper. While forecasting is the primary focus, to highlight the underlying nonlinear and time-varying relationship between growth and inflation with the ENSO to motivate the SSA across short-, medium- and long-runs, we also conduct an in-sample-based causality analysis using the wavelet coherence approach.

The remainder of the paper is organized as follows: Section 2 outlines the methodologies, while Section 3 presents the data and Section 4 discusses the results. Finally, Section 5 concludes.

2. Methods

The investigation of the impact of the ENSO on GDP growth and inflation is carried out in two stages. First a wavelet coherence analysis is used to investigate the complex relationship between the economic series and the ENSO. Next, we use a data driven forecasting method (mixed-frequency and standard multivariate SSA), and a nonparametric test (KSPA) to test for the role of monthly ENSO for quarterly GDP growth and monthly inflation. Following is a brief review of the employed methods.

2.1. Continuous Wavelet Transform and Coherence Analysis

A Continuous Wavelet Transform, CWT, uses a mother wavelet $\psi(.)$ to transform a discrete-time time series $\{y_t\}_1^n$, to wavelet daughters $W(\tau, s)$, for time localizing parameter τ and scale parameter s. The wavelet daughters $W(\tau, s)$ are defined as convolution of time series $\{y_t\}_1^n$ with the localized (in time and frequency space by τ

and s) mother wavelet $\psi(.)$ [4]:

$$W(\tau, s) = \sum_t y_t \frac{1}{\sqrt{s}} \bar{\psi}(\frac{t-\tau}{s}),$$

where $\bar{\psi}(.)$ is the complex conjugate of $\psi(.)$. Larger values of scale parameter s, reveal the long term periodic behavior (with low frequency) and smaller values of scale parameter reveal the details in short term periodic patterns (with higher frequencies). One common choice for mother wavelet is the Morlet wavelet [24]:

$$\psi(t) = \pi^{-1/4} e^{i\omega t} e^{-t^2/2},$$

where ω is dimension less frequency, also known as angular frequency. According to the literature, the $\omega = 6$ is the proper choice, since it makes the Morlet wavelet approximately analytic [4].

Large absolute values of $W(\tau, s)$ show the powerful periodic pattern in time τ and period s. The wavelet power spectrum of time series $\{y_t\}_1^n$ is defined as

$$Power(\tau, s) = \frac{1}{s} |W(\tau, s)|^2.$$

The power spectrum can be used to map the periodic patterns in the time series $\{y_t\}_1^n$, through time. The wavelet power spectrum can be tested against white noise spectrum, using asymptotic chi square statistic [10, 29] or Monte Carlo simulation [10, 29]. The Monte Carlo simulation approach is used in this paper.

In the bivariate case, the cross wavelet transform can be used to investigate the relation between two time series, x_t and y_t [4]:

$$W_{xy}(\tau, s) = \frac{1}{s} W_x(\tau, s) \bar{W}_y(\tau, s),$$

where $W_x(\tau, s)$ and $W_y(\tau, s)$ are the wavelet daughters in time series x_t and y_t, respectively and $\bar{W}$ denotes complex conjugate. The wavelet cross power spectrum can be used to map the similarities between two time series' periodic behavior:

$$Power_{xy}(\tau, s) = |W_{xy}(\tau, s)|.$$

Using the wavelet cross power spectrum, we can map the localized correlation between two series, through time and scale. Coherence between two time series x_t and y_t is defined as the local correlation between the series, localized at time τ and scale s [4]:

$$Coherence_{xy}(\tau, s) = \frac{|sW_{xy}(\tau, s)|^2}{sPower_x(\tau, s) Power_y(\tau, s)}.$$

Like power spectrum, wavelet Coherence between two series can be tested using Monte Carlo simulation [29].

2.2. *Standard and Mixed Frequency Multivariate Singular Spectrum Analyses*

Following is a brief review of implementing standard and mixed frequency MSSAs. Since the bivariate version of the method is used in this research, the notation is adapted to the two-variable case. Consider the bivariate time series $\{\boldsymbol{X}_t := (x_t, y_t)\}_{t\in\mathbb{S}}$, which takes values in $\mathcal{R}_{\boldsymbol{X}} \subseteq \mathbb{R}^2$. The index set $\mathbb{S}$ can be subset of either $\mathbb{Z}$ or $\mathbb{N}$. It is assumed that both series are already scaled appropriately and expressed in commensurable units of measurement. Using a observed time series of length n (i.e. $\boldsymbol{X}_1, ..., \boldsymbol{X}_n$) and embedding dimension L, MSSA follows these steps [19]:

(1) We apply the hankelization operator $\mathcal{H}_L(.)$ to each of the component series of $\boldsymbol{X}_t$, and obtain the trajectory $(m \times L)$ matrices $\boldsymbol{T}_i$ as:

$$\boldsymbol{T}_i := \mathcal{H}_L(X_{1i}, ..., X_{ni}), \quad i = 1, 2$$

where $X_{t1} = x_t$, $X_{t2} = y_t$ and $m = n-L+1$. Concatenate the trajectory matrices horizontally, and build the $(m \times 2L)$ MSSA trajectory matrix $\boldsymbol{T}_X := [\boldsymbol{T}_1, \boldsymbol{T}_2]$ which will be used for decomposition and reconstruction in next steps.

(2) We build the sample covariance matrix $\boldsymbol{C} := m^{-1}\boldsymbol{T}'_X\boldsymbol{T}_X$, which is block symmetric matrix, containing covariance and cross-covariance matrix for both component series of $\boldsymbol{X}_t$.

(3) Obtain eigenvalues $\lambda_1 \geq \cdots \geq \lambda_{2L}$ and eigenvectors $\boldsymbol{v}_1, \ldots, \boldsymbol{v}_{2L}$ of sample covariance matrix $\boldsymbol{C}$. Using eigenvalues and eigenvectors, one can decompose sample covariance matrix as:

$$\boldsymbol{C} = \sum_{j=1}^{2L} \lambda_j \boldsymbol{v}_j \boldsymbol{v}'_j = \boldsymbol{V}\boldsymbol{\Lambda}\boldsymbol{V}',$$

where $\boldsymbol{V}$ is a $(2L \times 2L)$ matrix containing all eigenvectors of $\boldsymbol{C}$.

(4) Partitioning $\boldsymbol{V}$ appropriately in to $\boldsymbol{V} = [\boldsymbol{V}'_1, \boldsymbol{V}'_2]'$, estimate the individual trajectory matrices as:

$$\hat{\boldsymbol{T}}_i(k) := \boldsymbol{T}_i\boldsymbol{Q}(k), \quad i = 1, 2,$$

where $\boldsymbol{Q}(k) := \sum_{i\in\mathcal{I}_k} \boldsymbol{v}_{ij}\boldsymbol{v}'_{ij}$ for a subset of eigenvectors in $\boldsymbol{V}$, i.e. $\mathcal{I}_k \subseteq \{1, ..., L\}$.

(5) Obtain the reconstructed series by applying diagonal averagein operator $\mathcal{D}_{(L,n)}(.)$ to the estimated trajectory matrices:

$$\left\{\hat{X}_{t,i}(k)\right\}_{t=1}^{n} := \mathcal{D}_{(L,n)}\left(\hat{\boldsymbol{T}}_i(k)\right)$$

Now, suppose the x_t is the time series observed in lower frequency (say quarterly) and y_t is the time series observed in higher frequency (say monthly). The mixed-frequency MSSA introduced by [20] follows these steps:

(1) We build the initial observation matrix in higher frequency by repeating the values in lower frequency. For instance, if x_t is observed quarterly (each observation is belongs to the end of the quarter) and y_t is monthly, the initial observation

matrix in monthly sampling frequency will be:

$$H^{(0)} = \begin{pmatrix} x_1 & y_1 \\ x_1 & y_2 \\ x_1 & y_3 \\ \hline x_2 & y_4 \\ x_2 & y_5 \\ x_2 & y_6 \\ \hline \vdots & \vdots \end{pmatrix}_{n\times 2}, I = \begin{pmatrix} 0 \\ 0 \\ 1 \\ \hline 0 \\ 0 \\ 1 \\ \hline \vdots \end{pmatrix}_{n\times 1},$$

where n is the number of observations in time series with higher frequency. As it can be seen, in each quarter, the monthly values in quarterly observed series, are filled-in with the end-of-the-quarter observation. The Matrix I shows which rows in matrix $H^{(0)}$ are actual quarterly observations (denoted as ones) and which ones are filled with end-of-the-quarter observation (denoted as zeros).

(2) Using a standard MSSA [19] on matrix $H^{(0)}$ to obtain the predicted values in higher frequency, namely $\hat{H}^{(0)}$. Initialize the root-mean-squared measure as the root mean square of first column in $\hat{H}^{(0)}$ (the column associated with the time series with lower sampling frequency):

$$RMSE^{(0)} = \sqrt{\frac{1}{n}\sum_{t=1}^{n}\left(\hat{h}_{t,1}^{(0)}\right)^2},$$

where $\hat{h}_{t,1}^{(0)}$ is the tth element in first column of $\hat{H}^{(0)}$.

(3) In ith iteration, we substitute actual observations (that is the second column of $H^{(0)}$ and the elements in first column which are the associated with ones in I matrix) into $\hat{H}^{(i-1)}$ and build the new H matrix:

$$H^{(i)} = \begin{pmatrix} \hat{h}_{t,1}^{(i-1)} & y_1 \\ \hat{h}_{t,2}^{(i-1)} & y_2 \\ x_1 & y_3 \\ \hline \hat{h}_{t,4}^{(i-1)} & y_4 \\ \hat{h}_{t,5}^{(i-1)} & y_5 \\ x_2 & y_6 \\ \hline \vdots & \vdots \end{pmatrix}_{n\times 2}.$$

(4) Applying standard MSSA to $H^{(i)}$ to obtain the new predicted values in higher frequency, namely $\hat{H}^{(i)}$.

(5) Obtaining a new root-mean-squared measure:

$$RMSE^{(i)} = \sqrt{\frac{1}{n}\sum_{t=1}^{n}\left(\hat{h}_{t,1}^{(i-1)} - \hat{h}_{t,1}^{(i)}\right)^2}.$$

(6) For some predefined small value ε, while $RMSE^{(i)} \leq RMSE^{(i-1)}$ and $|RMSE^{(i)} - RMSE^{(i-1)}| > \varepsilon$, we repeat steps (3) to (5).

(7) If $RMSE^{(i)} > RMSE^{(i-1)}$, consider the $\hat{H}^{(i-1)}$ as the final estimation for high frequency observation matrix and if $|RMSE^{(i)} - RMSE^{(i-1)}| \leq \varepsilon$, put $\hat{H}^{(i)}$ as final estimation for high frequency observation matrix.

(8) Applying standard MSSA on $\hat{H}$, the final estimation for high frequency observation matrix obtained in step (7),for out-of-sample forecasting.

2.3. Forecasting Evaluation

Suppose $E(y_{t+h}|\mathcal{F}_t)$ is the h step ahead forecast from MSSA and the η_{t+h} is the forecasting square error of the conditional mean model at time t:

$$\eta_{i+h} = (y_{t+h} - E(y_{t+h}|\mathcal{F}_t))^2 .$$

Kolmogorov-Smirnov Predictive Accuracy, KSPA, test [16] is used for comparing the forecasting accuracy of different models. Let $F_{\eta_{i+h}^{(k)}}(.)$ be the distribution function of square error corresponding to kth forecasting model. One tailed KSPA, tests the following hypothesis:

$$\begin{cases} H_0 : F_{\eta_{i+h}^{(1)}}(z) \leq F_{\eta_{i+h}^{(2)}}(z) \\ H_1 : F_{\eta_{i+h}^{(1)}}(z) > F_{\eta_{i+h}^{(2)}}(z) \end{cases} .$$

Rejection of the null hypothesis implies that the forecasting error of second model, $\eta^{(2)}$ is stochastically smaller than the forecasting error of the first model, $\eta^{(1)}$, i.e., the second forecasting model is significantly more accurate than the first one.

3. Data Description

As far as the metric of the ENSO cycle is concerned, traditionally the Southern Oscillation Index (SOI) index is used.[1] The SOI gives an indication of the development and intensity of El Niño or La Niña events in the Pacific Ocean. The SOI is calculated using the pressure difference between Tahiti and Darwin. Sustained negative (positive) values of the SOI below (above) 7(+ 7) often indicate El Niño (La Niña) episodes. Low atmospheric pressure tends to occur over warm water and high pressure occurs over cold water, in part because of deep convection over warm water. El Niño episodes are defined as sustained warming of the central and eastern tropical Pacific Ocean, and La Niña episodes are defined as sustained cooling of the central and eastern tropical Pacific Ocean, resulting in a decrease and an increase in the strength of the Pacific trade winds, respectively.

The reliability of the SOI, however, is considered limited due to both Darwin and Tahiti being well south of the equator, resulting in the surface air pressure at both locations being less directly related to ENSO. To overcome this issue, a new index called the Equatorial Southern Oscillation Index (EQSOI) has been created.[2] To generate the data for this index, two new regions centered on the equator are delimited, with

[1] See: `http://www.bom.gov.au/climate/enso/soi/`.

[2] See the discussion of Anthony Barnston of the National Oceanic and Atmospheric Administration here: `https://www.climate.gov/news-features/blogs/enso/why-are-there-so-many-enso-indexes-instead-just-one` for further details.

the western one located over Indonesia and the eastern one located over the equatorial Pacific, close to the South American coast. The EQSOI is obtained from the Climate Prediction Center (National Weather Service) of the National Oceanic and Atmospheric Administration (US Department of Commerce).[3] In our analysis, we use the EQSOI index to capture the ENSO.

As far as our macroeconomic variables are concerned, data on year-on-year growth of quarterly real GDP and monthly inflation rates of the US, other advanced barring the US and emerging market economies, as well as the overall World economy excluding the US are obtained from the Global Economic Database maintained by the Federal Reserve Bank of Dallas.[4] Data on 18 advanced (excluding the US, Japan, Germany, the United Kingdom (UK), France, Italy, Spain, Canada, South Korea, Australia, Taiwan, The Netherlands, Belgium, Sweden, Austria, Switzerland, Greece, Portugal, and Czech Republic, in order of Purchasing Power Parity (PPP)-adjusted GDP shares in 2005) and 21 emerging (China, India, Russia, Brazil, Mexico, Turkey, Indonesia, Poland, Thailand, Argentina, South Africa, Colombia, Malaysia, Venezuela, Philippines, Nigeria, Chile, Peru, Hungary, Bulgaria, and Costa Rica, in order of PPP-adjusted GDP shares in 2005) countries are used to compile the aggregates for the blocs, by using trade weights with the US in weighting the country-level data. The reader is referred to [13] for further details.

Based on latest data availability at the time of writing this paper, the monthly analysis involving the inflation rates and the EQSOI cover the period of February 1981 to July 2021, while the real GDP growth and EQSOI span the period of June 1981 (1981:Q2) to June 2021 (2021:Q2) for the US, the advanced and world economies excluding the US, but the same for emerging markets starts a bit later from March 1984 (1984:Q1), but also ends in June 2012 (2021:Q2).

4. Empirical Results

Before testing the role of EQSOI in forecasting inflation and GDP growth , we use CWT to investigate the underlying time-varying relation between EQSOI and the macroeconomic variables for each of the four economic areas. As a measure of dependency, EQSOI's wavelet coherence with inflation and GDP growth is estimated using CWT. For the GDP growth case, since we are interested in coherence between the monthly EQSOI and the quarterly GDP growth, the sampling frequency for the monthly series is set to 3 (i.e., 3 samples during each quarter), so the time unit in the wavelet figures will correspond to a quarter. Latter, in mixed-frequency MSSA (MFMSSA), we will use the original monthly data to forecast the quarterly GDP.

We use MSSA to forecast inflation and MFMSSA to forecast GDP growth when EQSOI is included as a predictor. For each economic area, two sets of forecasts are produced: one without using any predictor, and one using EQSOI as a predictor. Specifically, following is the list of forecasting models:

- Model 1: Forecasting inflation without any predictors; i.e., univariate forecasts using SSA.
- Model 2: Forecasting inflation using EQSOI as a predictor; i.e., bivariate forecasts using MSSA.
- Model 3: Forecasting GDP growth without any predictors; i.e., univariate fore-

[3] https://www.cpc.ncep.noaa.gov/data/indices/.

[4] https://www.dallasfed.org/institute/dgei/gdp.aspx.

casts using SSA.

- Model 4: Forecasting GDP growth using SOI as predictors; i.e., bivariate forecasts using MFMSSA.

Since SSA can be used with even non-stationarity data [11, 21, 22], unit root tests are not necessary to be conducted to ensure stationarity before resorting to forecasting using SSA. The KSPA test is employed to compare the accuracy of the forecasts with and without the predictor. In this regard, the null and alternative hypotheses, for comparing univariate and bivariate models associated with the KSPA test are as follows:

(1) For comparing Model 1 and Model 2 (testing for EQSOI's role in inflation forecasting):

$$\begin{cases} H_0 : F_{\eta^{(1)}_{i+h}}(z) \leq F_{\eta^{(2)}_{i+h}}(z) \\ H_1 : F_{\eta^{(1)}_{i+h}}(z) > F_{\eta^{(2)}_{i+h}}(z) \end{cases} ; \tag{1}$$

(2) For comparing Model 3 and Model 4 (testing for EQSOI's role in GDP growth forecasting):

$$\begin{cases} H_0 : F_{\eta^{(3)}_{i+h}}(z) \leq F_{\eta^{(4)}_{i+h}}(z) \\ H_1 : F_{\eta^{(3)}_{i+h}}(z) > F_{\eta^{(4)}_{i+h}}(z) \end{cases} ; \tag{2}$$

where $\eta^{(i)}_{i+h}$ is the h-step ahead forecasting square error corresponding to "Model i".

In each case, half of the data is used for estimating the SSA/(MF)MSSA, and the rest is used for out-of-sample forecasting, with the KSPA test applied to the out-of-sample forecasting results (with significance level set at: $\alpha = 0.05$). Rejecting the null hypothesis in 1 implies that Model 2 (inflation forecasting model containing EQSOI as predictor) dominates Model 1 (univariate inflation forecasting) significantly. In the same manner, rejecting the null hypothesis in 2 implies that Model 3 (GDP growth forecasting model containing EQSOI as predictor) dominates the null model (univariate GDP growth forecasting) significantly.

4.1. Inflation Forecasting Results

Figures 1 and 2 show the monthly EQSOI and inflation time series for the four economic blocs. As can be seen, there are resemblance among the inflation time series, especially around 2008 during the Global Financial Crisis (GFC).

In order to better understand the similarities in the periodic behavior of EQSOI and inflation, a CWT is used to estimate their power spectrums over time. The estimated power spectrums are shown in figures 3 and 4. Black contours present significant power spectrums. EQSOI's power spectrum shows significant periodic behavior with the periodic length falling between 16 and 64 months, as well as periods with length around 128 months. The significant periods of EQSOI are almost steady (i.e., almost the same) over time.

Figure 4 shows the wavelet power spectrum for inflation in advanced economies (with US excluded) (top left), emerging economies (top right), the US economy (bottom left) and the world economy (with US excluded) (bottom right). As Figure 4 shows, the inflation in advanced, the US and the world economies have significant periodic

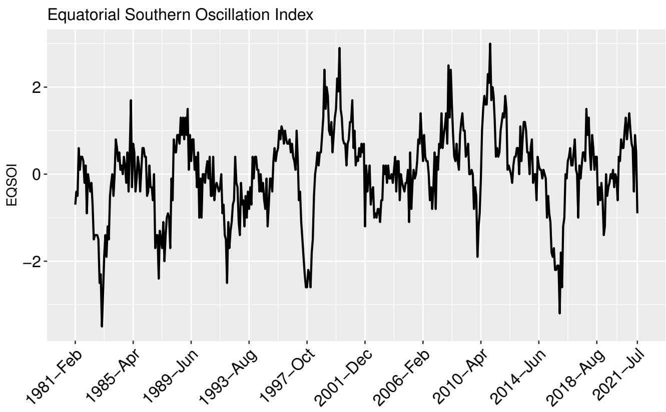

Figure 1. Monthly Equatorial Southern Oscillation Index time series.

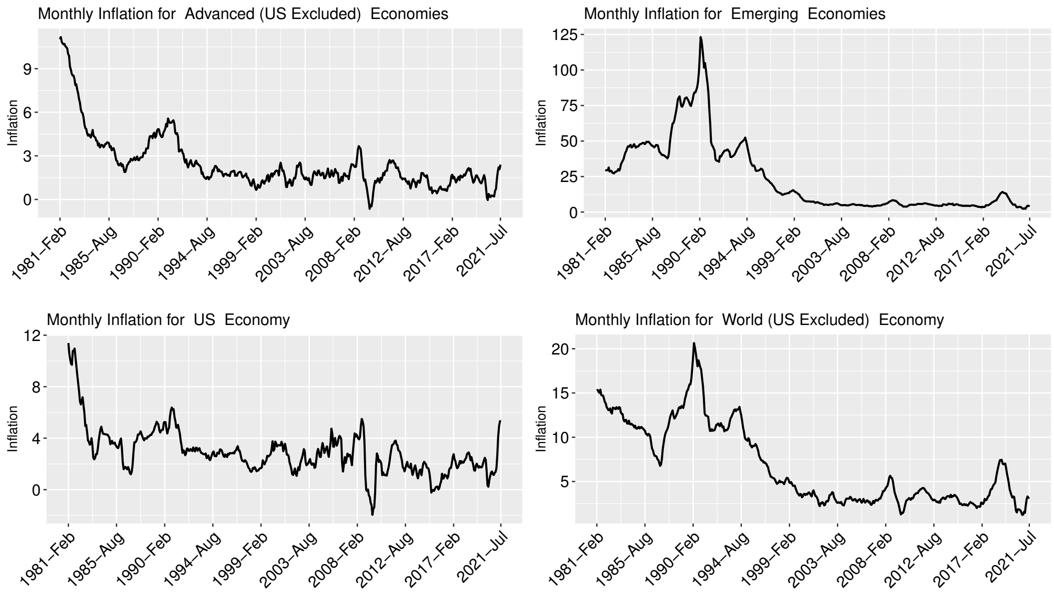

Figure 2. Top Left: Monthly Inflation time series in "Advanced Economies" (US excluded); Top Right: Monthly Inflation time series in "Emerging Economies"; Bottom Left: Monthly Inflation time series in "US Economy"; Bottom Right: Monthly Inflation time series in "World Economy" (US excluded).

behavior mostly between 32 and 128 month periods, which overlaps with those of the EQSOI's significant periods. For emerging economies however, there is no evidence of significant period in recent years (i.e., after 2011).

According to wavelet power spectrums, EQSOI and inflation have resemblance in their periodic behavior, in three economic areas i.e., advanced (without the US), the US and the world (with the US excluded) economies. Given this, we can suggest that, if significant correlation between the EQSOI and inflation is observed in same periods (i.e., the location where the power spectrum is significant for both EQSOI and inflation), we may be able to use one time series as a predictor to forecast the other one.

As a measure of correlation between the inflation and EQSOI, the wavelet coherences are presented in Figure 5. According to these results, there is significant wavelet

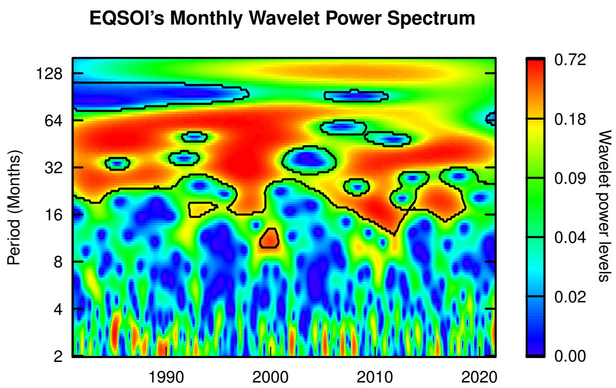

Figure 3. Equatorial Southern Oscillation (EQSOI) Index continuous monthly wavelet power spectrum. The thick black contour designates the 10% significance level.

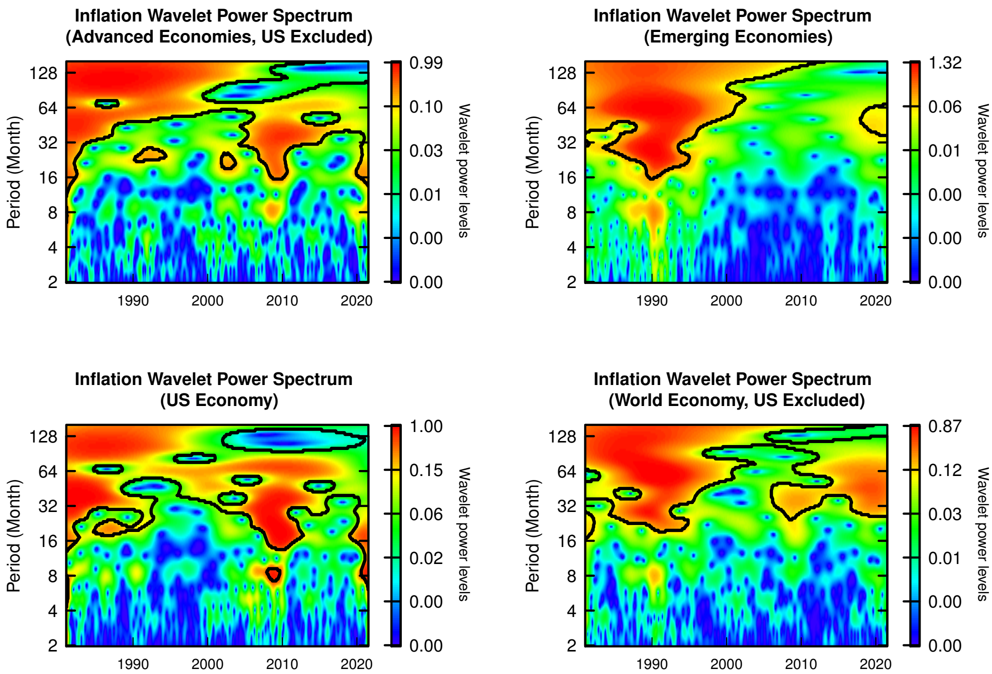

Figure 4. Top Left: Inflation's wavelet power spectrum in "Advanced Economies" (US excluded). Top Right: Inflation's wavelet power spectrum in "Emerging Economies". Bottom Left: US Inflation's wavelet power spectrum. Bottom Right: World Inflation's wavelet power spectrum (US excluded). The thick black contour designates the 10% significance level.

coherence between EQSOI and inflation (green, yellow and red areas show coherence above 0.94), though not significant in most of the periods over time. The significant wavelet coherence between EQSOI and Inflation occurs mostly around 32- and 64-month periods, in all four economic areas. However, as it is evident form Figure 5, the significant coherence between EQSOI and inflation does not always correspond to the location (i.e., for time and periods) with highest power spectrum. For instance, in emerging economies, inflation's power spectrum around the 32-month period is not significant after 2000. This means that the period in which EQSOI and inflation have significant coherence, is a period which has low power (and hence low impact) on inflation's periodic pattern. In the case, where significant coherence between inflation and EQSOI fall in the periods with high values of wavelet power spectrum in both series, we may use EQSOI as a potential predictor for inflation forecasting (provided oscillations in EQSOI occur before inflation). But as is well-known, existence of in-sample causality cannot guarantee that the same will hold over an out-of-sample, since the latter is stronger test of predictability, and we consider this next.

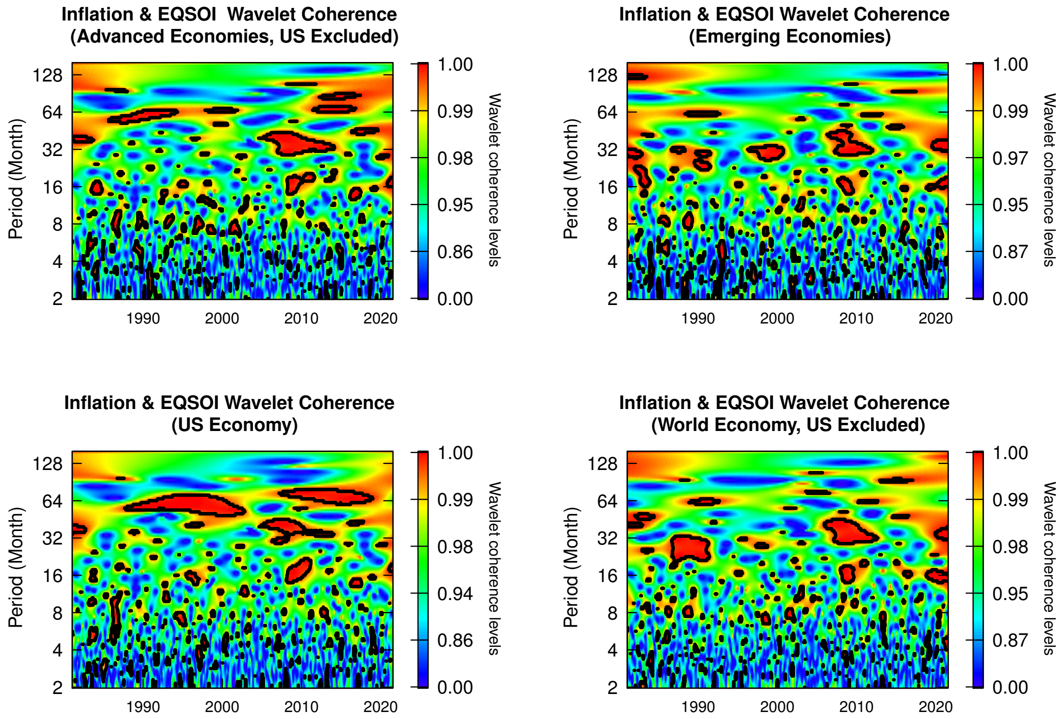

Figure 5. Top Left: Wavelet coherence between Inflation in "Advanced Economies" (US excluded) and SOI. Top Right: Wavelet coherence between Inflation in "Emerging Economies" and SOI. Bottom Left: Wavelet coherence between US Inflation and SOI. Bottom Right: Wavelet coherence between World Inflation (US excluded) and SOI. The 10% significance level is shown as a thick black contour.

KSPA p-values for testing the role of EQSOI in forecasting inflation (i.e., hypothesis (1)), for four economic areas, are presented in Table 1. According to KSPA test results, using EQSOI as predictor can significantly improve inflation forecasting accuracy (i.e., rejects the null hypothesis in (1)) for medium- and long-term forecasting horizons, in advanced and world economies (with US excluded), as well as for the US economy (i.e., $h \geq 10$ in advanced economies, $h \geq 9$ in the US economy and $h \geq 7$ in world economy). In emerging economies, however, using EQSOI as predictor does not improve inflation forecasting accuracy (i.e., the null hypothesis in (1) is not rejected).

4.2. GDP Growth Forecasting Results

Figure 6 shows the quarterly GDP growth for the four economic areas. As it can be seen, there are similarities between the EQSOI (as presented in Figure 1) and the GDP growth rates, again especially during the GFC, just as in case of the inflation

Table 1. KSPA test p-values for testing the EQSOI effect on inflation forecasting accuracy, Hypothesis (1).

Forecasting Horizon	Advanced Economies (US excl.)	Emerging Economies	US Economy	World Economy (US excl.)
$h = 1$	1.0000	1.0000	0.9299	0.8926
$h = 2$	0.9820	0.9955	0.8926	0.5197
$h = 3$	0.9955	1.0000	0.5769	0.7476
$h = 4$	1.0000	1.0000	0.4103	0.6920
$h = 5$	0.8926	0.9955	0.2293	0.2293
$h = 6$	0.6920	1.0000	0.0729	0.0584
$h = 7$	0.6347	1.0000	0.1623	**0.0127***
$h = 8$	0.2688	1.0000	0.0584	**0.0007***
$h = 9$	0.0903	1.0000	**0.0127***	**0.0167***
$h = 10$	**0.0052***	1.0000	**0.0127***	**0.0167***
$h = 11$	**0.0014***	0.9955	**0.0002***	**0.0071***
$h = 12$	**0.0000***	1.0000	**0.0000***	**0.0020***
$h = 13$	**0.0001***	1.0000	**0.0014***	**0.0007***
$h = 14$	**0.0000***	1.0000	**0.0001***	**0.0038***
$h = 15$	**0.0000***	1.0000	**0.0003***	**0.0005***
$h = 16$	**0.0000***	1.0000	**0.0002***	**0.0001***
$h = 17$	**0.0000***	1.0000	**0.0000***	**0.0002***
$h = 18$	**0.0000***	1.0000	**0.0000***	**0.0001***
$h = 19$	**0.0000***	1.0000	**0.0000***	**0.0000***
$h = 20$	**0.0000***	1.0000	**0.0003***	**0.0000***
$h = 21$	**0.0000***	0.9955	**0.0003***	**0.0000***
$h = 22$	**0.0000***	0.9599	**0.0000***	**0.0000***
$h = 23$	**0.0000***	0.9599	**0.0002***	**0.0001***
$h = 24$	**0.0000***	0.9599	**0.0002***	**0.0000***

.* EQSOI improves the inflation forecasting accuracy, significant(at $\alpha = 0.05$ level).

rates.

Figure 7 shows the quarterly measured wavelet power spectrum for the EQSOI (with the sampling frequency set to 3 in time unit, since there are three monthly observations in each quarter). Significant power spectrums are shown with black contour lines. As the EQSOI's wavelet power spectrum shows, there are significant mid- and long-range (longer than 8 quarters) periodic pattern in the EQSOI, which is basically the same as the monthly measured power spectrum (presented in Figure 3).

Figure 8 shows the wavelet power spectrum for GDP growth in "Advanced Economies (US excluded)", (top left), "Emerging Economies" (top right), "US Economy" (bottom left) and "World Economy (US excluded)" (bottom right). As it can be seen in Figurer 8, steady GDP growth significant periodic patterns mostly fall in the midrange (between 8 and 16 quarters) and long periods (around 32 quarters), which overlaps with the EQSOI's periodic pattern, especially in mid-range periods. In general, the GDP growth power spectrums in all four economic areas show significant periodic behavior that has similarities with the EQSOI through time.

The wavelet coherences between the GDP growth rates and the EQSOI are presented in Figure 9. Figure 9, shows that there is high wavelet coherence between the

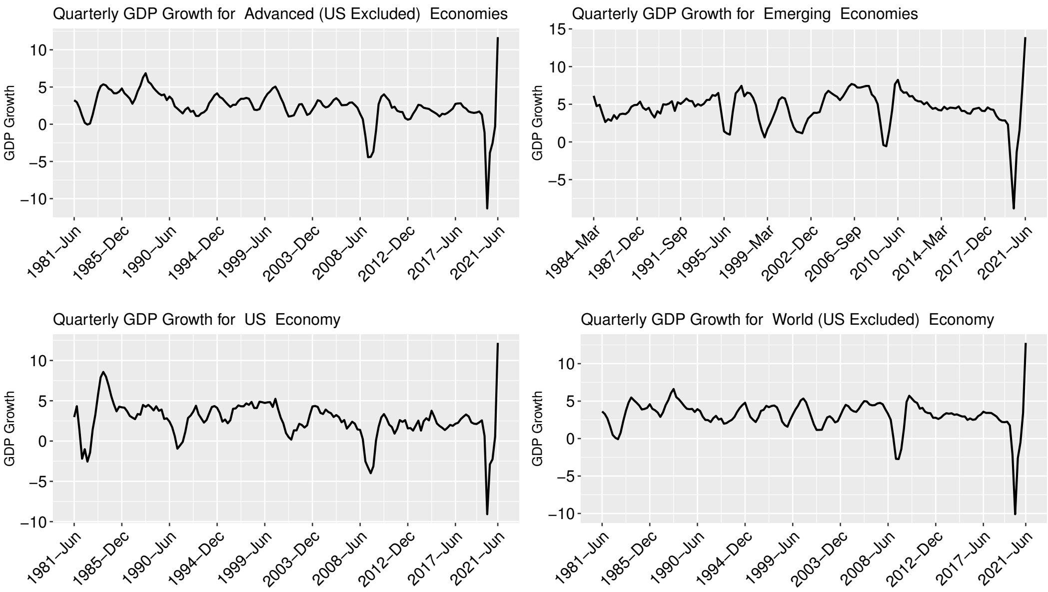

Figure 6. Quarterly GDP growth time series for "Advanced Economies (US excluded)", top left; "Emerging Economies", top right; "US Economy", bottom left; "World Economy (US excluded)", bottom right.

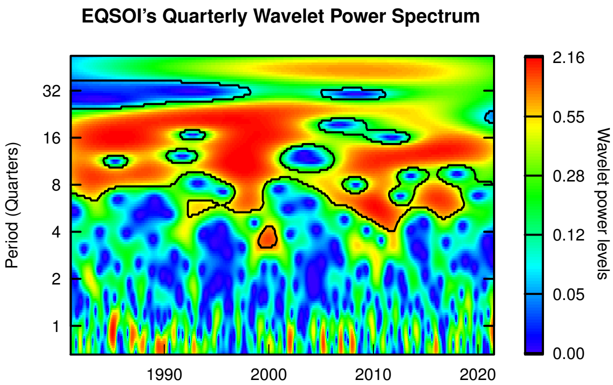

Figure 7. Equatorial Southern Oscillation (EQSOI) Index continuous quarterly wavelet power spectrum; The thick black contour designates the 10% significance level.

EQSOI and GDP growth rates (green, yellow and red areas show coherence above 0.94). However, the significant wavelet coherence between the EQSOI and the GDP growth occur mostly in midrange periods (around 8 and 16 quarters), in all economic areas. Furthermore, according to Figure 9, the coherence between EQSOI and the GDP growth is observed to be stronger before 2000s in the "Advanced Economies", the "US Economy" and the "World Economy", as evident from large red areas on the left side of time axis in the top left, the bottom left and the bottom right panels of Figure 9. According to CWT results, as is evident from figures 8 and 9, the GDP growth have similarities with EQSOI in power spectrums, and there exist significant wavelet coherence between them. Since the significant coherence between the two series is located in the areas with significant power spectrum in both series, the EQSOI can be considered as a potential predictor in forecasting GDP growth rates, but for

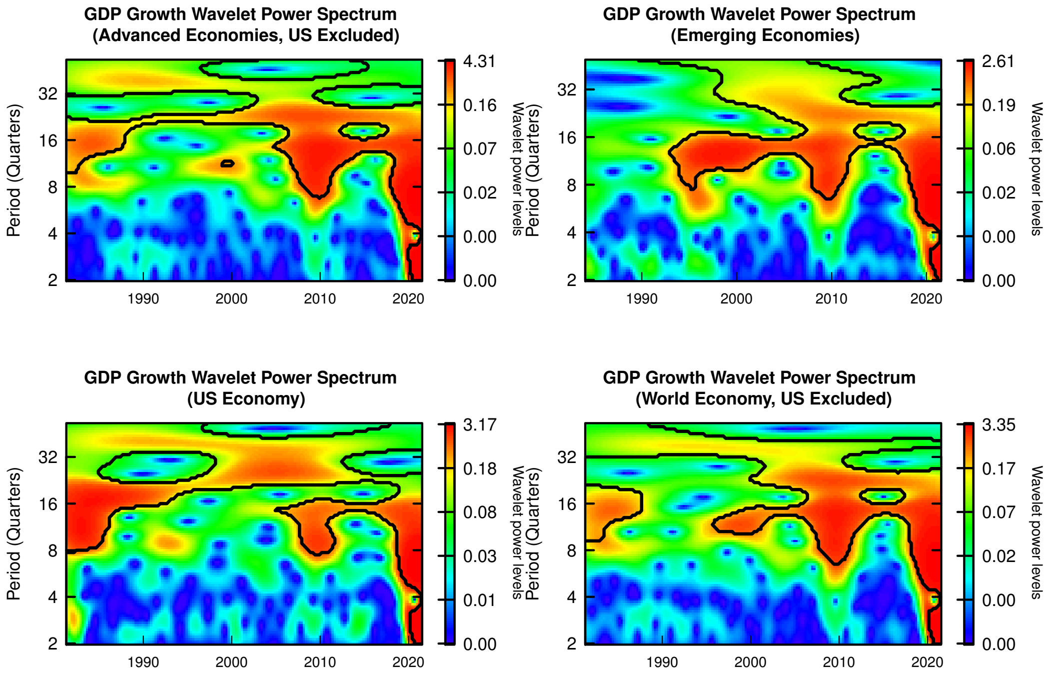

Figure 8. GDP growth wavelet power spectrum for "Advanced Economies (US excluded)", top left; "Emerging Economies", top right; "SU Economy", bottom left; "World Economy (US excluded)", bottom right; The thick black contour designates the 10% significance level.

this to happen, the oscillation in the EQSOI need to occur well enough before it is observed in the GDP growth rates. But again in-sample predictability is no guarantee for out-of-sample forecasting gains, and it is the latter which we turn to next.

Table 2 show the results of quarterly GDP growth forecasting using SSA and MFMSSA with and without EQSOI as predictor respectively. As can be seen, the bivariate forecasting model (the model using EQSOI as a predictor) significantly improves the GDP growth forecasting accuracy in advanced and world economies (with US excluded), mostly at the short-term, and also at certain medium- and long-run horizons (i.e. $h = 1$, ..., 6, 16, 24 for the former, and $h = 1$, ..., 8, 15 and 16 for the latter). For emerging economies, EQSOI significantly improves GDP growth forecasting accuracy at very short ($h = 1$) and medium-term ($h = 14$, ..., 17) horizons. Interestingly for the US GDP growth forecasting, EQSOI as predictor does not provide significant forecasting gains at any horizon.

5. Conclusion

In this paper, for the first time, the role of the ENSO, as captured by the EQSOI index is used to formally forecast the inflation and GDP growth rates of not only the US economy, but advanced (excluding the US) and emerging countries, as well as for the world economy (barring the US). For our purpose, we use univariate and multivariate SSA, as well as mixed-frequency version of the latter since the EQSOI is monthly, while GDP growth is available only at quarterly frequency unlike monthly inflation rates.

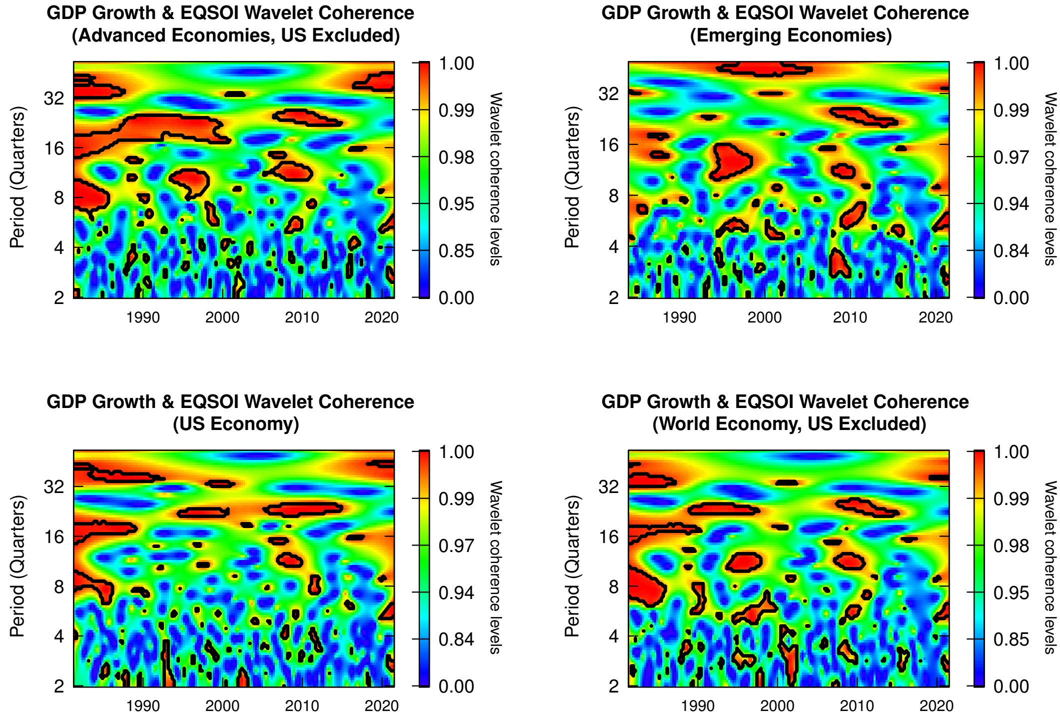

Figure 9. Wavelet coherence between GDP growth and SOI. "Advanced Economies (US excluded)", top left; "Emerging Economies", top right; "SU Economy", bottom left; "World Economy (US excluded)", bottom right; The 10% significance level is shown as a thick black contour.

As a preliminary analysis to motivate the use of the SSA method which is a model-free approach, we also use the wavelet coherence to depict complex time-varying relationships between the macro variables and the EQSOI. Since in-sample predictability does not guarantee the same for the out-of-sample, we then turned to the SSA method to show that the EQSOI significantly improves the forecasting accuracy of the inflation rates at medium- and long-runs for the advanced and world economies (when the US is excluded), as well as for the US economy. For inflation rate of the emerging economies however, the use of the EQSOI as predictor does not produce forecasting gains. At the same time, GDP growth forecasting results show that using the EQSOI as predictor significantly improves accuracy in advanced (with US excluded) and emerging countries, as well as for the world economy (excluding the US). For these country groups, the improvement is mostly evident in short horizons, as well as certain medium and long-runs for advanced and world economies (when US is excluded), and very short as well as for the medium-term associated with emerging economies. Interestingly, using EQSOI as predictor does not improve the forecasting accuracy of US GDP growth. In sum, the ENSO tend to predict both in- and out-of-sample inflation and GDP growth rates globally, though there are exceptions in terms of forecasting of the inflation rate of emerging economies and the growth rate of the US. These contrasting results for the emerging markets and the US in terms of forecastability of output growth and inflation respectively emanating from the EQSOI, seems to be indicative of the strong reliance of emerging countries on agriculture (and its corresponding high share in GDP), and the US being the highest importer in the overall of commodity market.

Table 2. KSPA test p-values for testing the SOI effect on GDP growth forecasting accuracy, Hypothesis (2).

Forecasting Horizon	Advanced Economies (US excl.)	Emerging Economies	US Economy	World Economy (US excl.)
$h = 1$	**0.0034** *	**0.0000***	0.6449	**0.0000***
$h = 2$	**0.0018** *	0.0594	0.4233	**0.0063***
$h = 3$	**0.0063** *	0.6125	0.6449	**0.0009***
$h = 4$	**0.0002** *	0.3826	0.1730	**0.0034***
$h = 5$	**0.0034** *	0.4937	0.4233	**0.0002***
$h = 6$	**0.0321** *	0.4937	0.4233	**0.0009***
$h = 7$	0.2415	0.4937	0.6449	**0.0063***
$h = 8$	0.5318	0.6125	0.4233	**0.0321***
$h = 9$	0.6449	0.4937	0.3254	0.0516
$h = 10$	0.6449	0.2851	0.7553	0.0516
$h = 11$	0.7553	0.2043	0.6449	0.0516
$h = 12$	0.3254	0.1407	0.6449	0.0516
$h = 13$	0.2415	0.0932	0.9322	0.0516
$h = 14$	0.3254	**0.0364***	0.8539	0.0516
$h = 15$	0.3254	**0.0364***	0.8539	**0.0018***
$h = 16$	**0.0193***	**0.0364***	0.4233	**0.0112***
$h = 17$	0.0800	**0.0214***	0.4233	0.0516
$h = 18$	0.1197	0.1407	0.4233	0.1197
$h = 19$	0.5318	0.3826	0.6449	0.1197
$h = 20$	0.6449	0.2043	0.8539	0.2415
$h = 21$	0.3254	0.3826	0.9322	0.4233
$h = 22$	0.3254	0.3826	0.9322	0.7553
$h = 23$	0.1730	0.2851	0.9322	0.5318
$h = 24$	**0.0321***	0.2043	0.8539	0.6449

.* EQSOI improves GDP growth forecasting accuracy, significant (at $\alpha = 0.05$ level).

Clearly, these findings associated with forecasts of inflation and growth due to the El Niño and La Ninña events will allow policymakers to design monetary policy decisions to circumvent business cycle downturns and inflationary episodes.

As part of future research, it would be interesting to extend our analysis to study individual countries rather than advanced and emerging economies as blocs, since there is lot of heterogeneity within these countries. Furthermore, one can also analyze the role of the ENSO cycle for forecasting asset prices, given that climate risks are known to affect financial markets [12].

References

[1] Brunner, A.D. (2002). El Niño and World Primary Commodity Prices: Warm Water or Hot Air? *Review of Economics and Statistics*, **84**(1), 176–183; DOI: 10.1162/003465302317332008

[2] Berry, B., and Okulicz-Kozaryn, A. (2008). Are there ENSO signals in themacroeconomy? Ecological Economics, **64**(3), 625-633; DOI: 10.1016/j.ecolecon.2007.04.009

[3] Campbell, J.Y. (2008). Viewpoint: estimating the equity premium. *Canadian Journal of*

Economics, **41**, 1–21; DOI: 10.1111/j.1365-2966.2008.00453.x

[4] Carmona, R., Hwang, W.L., and Torresani, B. (1998). *Practical Time Frequency Analysis: Gabor and Wavelet Transforms with an Implementation in S.* Academic Press: San Diego.

[5] Cashin, P., Mohaddes, K., and Raissi, M. (2017). Fair weather or foul? The macroeconomic effects of El Niño. *Journal of International Economics*, **106**, 37–54; DOI: 10.1016/j.jinteco.2017.01.010

[6] Changnon, S.A. (1999). Impacts of 1997–98 El Niño generated weather in the United States. *Bulletin of the American Meteorological Society*, **80**, 1819–1827; DOI: 10.1175/1520-0477(1999)080¡1819:IOENOG¿2.0.CO;2

[7] Davis, M. (2001). *Late Victorian Holocausts: El Niño Famines and the Making of the Third World*. London, UK: Verso.

[8] Das, S., Demirer, R., Gupta, R., Mangisa, S. (2019). The effect of global crises on stock market correlations: Evidence from scalar regressions via functional data analysis. *Structural Change and Economic Dynamics*, **50**(C), 132–147; DOI: 10.1016/j.strueco.2019.05.007

[9] De Winne, J., and Peersman, G. (2021). The adverse consequences of global harvest and weather disruptions on economic activity. *Nature Climate Change*, **11**, 665–672; DOI: 10.1038/s41558-021-01102-w

[10] Ge, Z. (2007). Significance tests for the wavelet power and the wavelet power spectrum. *Annales Geophysicae*, **25**, 2259–2269; DOI: 10.5194/angeo-25-2259-2007

[11] Ghodsi, M., Hassani, H., Rahmani, D., and Silva, E.S. (2018). Vector and recurrent singular spectrum analysis: Which is better at forecasting? *Journal of Applied Statistics*, **45**, 1872–1899; DOI: 10.1080/02664763.2017.1401050

[12] Giglio, S., Kelly, B., and Stroebel, J. (2021). Climate Finance. *Annual Review of Financial Economics*, **13**; DOI: 10.1146/annurev-financial-102620-103311

[13] Grossman, V., Mack, A., and Martnez-Garca, E. (2014). Database of Global Economic Indicators (DGEI): A Methodological Note. *Journal of Economic and Social Measurement*, **39**(3), 163–197; DOI: 10.3233/JEM-140391

[14] Grove, R.H. and Chappell, J. (2000). *El Niño–History and Crisis*. Cambridge, UK: The White Horse Press.

[15] Hassani, H., Silva, E.S., Gupta, R., and Segnon, M.K. (2015). Forecasting the price of gold. *Applied Economics*, **47**(39), 4141–4152; DOI: 10.1080/00036846.2015.1026580

[16] Hassani, H., and Silva, E.S. (2015). A Kolmogorov-Smirnov based test for comparing the predictive accuracy of two sets of forecasts. *Econometrics*, **3**, 590–609; DOI: 10.3390/econometrics3030590

[17] Hassani, H., Ghodsi, Z., Gupta, R., and Segnon, M.K. (2017). Forecasting Home Sales in the Four Census Regions and the Aggregate US Economy Using Singular Spectrum Analysis. *Computational Economics*, **49**, 83–97; DOI: 10.1007/s10614-015-9548-x

[18] Hossein, H., Silva, E.S., and Gupta, R., and Das S. (2018). Predicting global temperature anomaly: A definitive investigation using an ensemble of twelve competing forecasting models. *Physica A: Statistical Mechanics and its Applications*, **509**, 121–139; DOI: 10.1016/j.physa.2018.05.147

[19] Hassani, H., and Mahmoudvand, R. (2018). Multivariate Singular Spectrum Analysis. In: *Singular Spectrum Analysis: Using R*. Palgrave Advanced Texts in Econometrics; Palgrave Pivot: London; DOI: 10.1057/978-1-137-40951-5_2

[20] Hassani, H., Rua, A., Silva, E.S., and Thomakos, D. (2019). Monthly forecasting of GDP with mixed-frequency multivariate singular spectrum analysis. *International Journal of Forecasting*, **35**, 1263–1272; DOI: 10.1016/j.ijforecast.2019.03.021

[21] Hassani, H., Yeganegi, M.R., Khan, A., and Silva, E.S. (2020). The effect of data transformation on singular spectrum analysis for forecasting. *Signals*, **1**, 4–25; DOI: 10.3390/signals1010002

[22] Hassani, H., Yeganegi, M.R., and Huang, X. (2021). Fusing nature with computational science for optimal signal extraction. *Stats*, **4**, 71–85; DOI: 10.3390/stats4010006

[23] Laosuthi, T., and Selover, D.D. (2007). Does El Niño affect Business Cycles? *Eastern*

Economic Journal, **33**(1), 21–42; DOI: 10.1057/eej.2007.2

[24] Morlet, J., Arens, G., Fourgeau, E., and Giard, D. (1982). Wave propagation and sampling theory – Part I: complex signal and scattering in multilayered media. *Geophysics*, **47**, 203–221; DOI: 10.1190/1.1441328

[25] Peersman, G. (2020). International food commodity prices and missing (dis)inflation in the euro area. *The Review of Economics and Statistics*; DOI: 10.1162/rest_a_00939.

[26] Qin, M., Qiu, L-H., Tao, R., Umar, M., Su, C-W., and Jiao, W. (2020) The inevitable role of El Niño: A fresh insight into the oil market. *Economic Research–Ekonomska Istraživanja*, **33**(1), 1943–1962; DOI: 10.1080/1331677X.2020.1768428

[27] Sanei, S., and H. Hassani. (2015). *Singular Spectrum Analysis of Biomedical Signals*. United States: CRC Press.

[28] Smith, S., and Ubilava, D. (2017). The El Niño-Southern Oscillation and economic-growth in the developing world. *Global Environmental Change*, **45**, 151-164; DOI: 10.1016/j.gloenvcha.2017.05.007

[29] Torrence, C., and Compo, G.P. (1998). A practical guide to wavelet analysis. *Bulletin of the American Meteorological Society*, **79**, 61–78; DOI: https://doi.org/10.1175/1520-0477(1998)079¡0061:APGTWA¿2.0.CO;2

[30] Trenberth, K.E., Jones, P.D., Ambenje, P., Bojariu, R., Easterling, D., Tank, K.A., Parker, D., Rahimzadeh, F., Renwick, J.A., Rusticucci, M., Soden, B., and Zhai, P. (2007). Observations: Surface and Atmospheric Climate Change. S. Solomon, D. Qin, M. Manning, Z. Chen, M. Marquis, K.B. Averyt, M. Tignor and H.L. Miller (eds.). *Climate Change 2007: The Physical Science Basis. Contribution of Working Group I to the Fourth Assessment Report of the Intergovernmental Panel on Climate Change*. Cambridge, UK: Cambridge University Press. 235–336.